Chapter 8

Evaluation of model performance

8.1 Overview of match between measurements and simulations

The central focus of this thesis has been on the ability of musculo-skeletal modelling to predict patterns of torque applied to the cranks of an isokinetic cycle ergometer. Prediction of crank torques requires the model to generate appropriate muscle forces in response to NMES, joint torques resulting from the muscle forces and pedal forces resulting from the interaction between joint torques and segmental kinematics. Crank torques are therefore analysed here because they require a synthesis of all components of the model. Detailed comparisons between modelled and measured crank torques have already been described in Chapter 7. The purpose of this overview is not simply to summarise the comparisons that have already been made for individual muscles. Rather the intent is to make comparisons between muscles to highlight the major strengths and weaknesses of the present model.

Figure 8.1.1 illustrates modelled and measured crank torques from a single set of stimulation firing angles for each muscle group. These particular firing angles have been chosen for illustration here because they contain a small period of negative crank torque prior to the production of positive torque. This negative period allows identification of the crank angle where torque first becomes positive. For the model to accurately predict peak stimulation firing angles, it must be able to predict both this initial positive angle as well as the delay between stimulation onset and the application of force to the pedals.

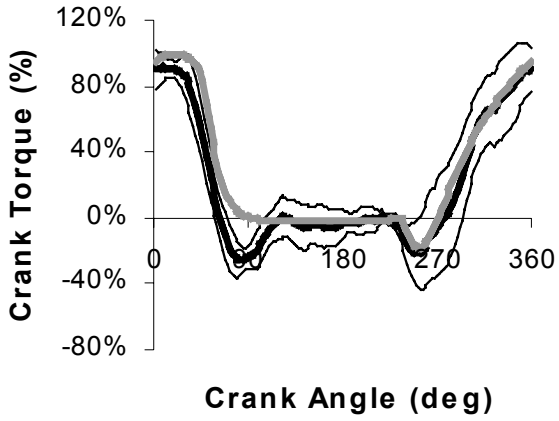

a) quadriceps 220 deg onset

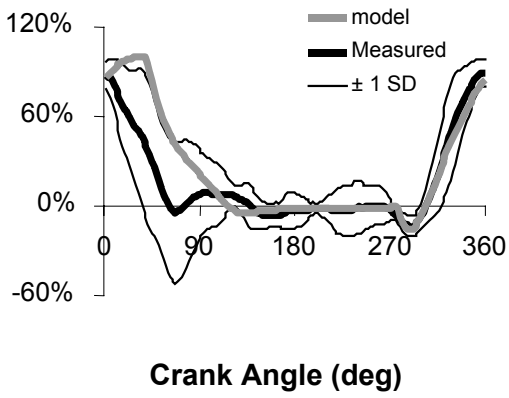

b) gluteals 260 deg onset

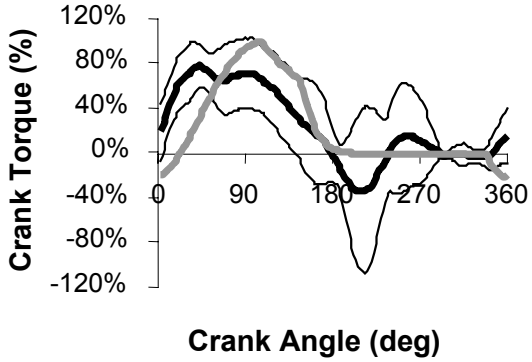

c) hamstrings 320 deg onset
original moment arms

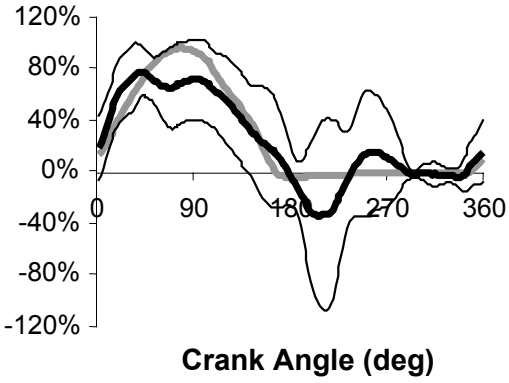

d) hamstrings 320 deg onset
modified moment arms

Figure 8.1.1 Comparison between measured and modelled crank torques for quadriceps, hamstring and gluteal muscles.

Time of torque development in response to stimulation.

The time when crank torque was first generated in response to stimulation was well predicted by the model for all muscle groups (Figure 8.1.1). The timing parameters that were used to model all muscle groups were derived from experimental measurements taken only from the quadriceps muscles at a 60 deg knee angle. While discussion within Sections 5.1.1 and 7.6

suggests that the duration of the delay period is sensitive to such factors as tendon slack length and muscle length at the time of stimulation onset, it appears that these differences have only a minor effect on the present results. The use of a single delay constant thus enables the model to predict appropriate torque rise times within the variance of measured responses for all three muscle groups.

Initial rise of torque in response to stimulation onset

The quadriceps and gluteal muscles demonstrate a good match between measured and modelled crank torques during the initial rise of torque (Figure 8.1.1). The model predicts both the magnitude and direction of the initial torque change for these muscles and thus predicts those firing angles that would result in negative torque. For those trials where crank torque was initially negative, the model predicted the angle where torque would cross over to positive values.

The results for hamstring muscles were less clear. Variance between individuals meant that the angles where crank torque was negative differed between subjects. It was proposed in Section 7.3 that at least part of this variability resulted from individual differences in the ratio between hip and knee moment arms. Those subjects with a larger moment arm at the knee did not produce positive crank torques in response to stimulation until a later crank angle. At TDC, the original model predicted that stimulation of the hamstring group would apply negative torque to the crank, while average measured torques were positive at this time (Figure 8.1.1c). Modifications of the model's hamstring moment arm across the knee for individual subjects greatly improved the model's accuracy during the early rise of crank torque (Figure 8.1.1d).

Time of peak torque

The time of peak crank torque was well predicted for quadriceps muscles, but not for the hamstrings or gluteals. This probably indicates that the model did not predict joint torque-angle torque curves with sufficient precision (see Sections 6.1.2 and 6.2). For gluteus maximus, the model was overly simplistic, using a single fibre to represent a muscle with such a broad origin. Excessive fibre excursion required by this single fibre meant that the model could not generate torque over the full range of hip angles that are active in-vivo.

Modelling the hamstrings is more complicated because they act across both the hip and knee joints. Therefore, the pattern of crank torque by these muscles depends not only on the pattern of torque-angle curves, but also on the relative magnitude of torques generated about these joints. That is, even when the model can predict the general pattern of joint torques generated (eg Figure 6.2.1.2), an inappropriate ratio of hip to knee moment arms for the hamstring muscles would cause inaccurate crank torques to be predicted by the model. Figure 8.1.1 c&d shows that modifying the moment arm ratio for individual subjects improves the match between measured and modelled torques. It should be noted that the large inter-subject variance means that the averaged curves in Figure 8.1.1 may not necessarily be representative of any particular subject. Individual subjects' results may be seen in Figures 7.3.1.6 and 7.3.1.9.

Decline of torque after stimulation cessation

The design of the cycle ergometer used in these experiments prevented decisive comparisons from being made between measured and modelled crank torques during the declining portion of the torque production phase. The measured crank torque declined sooner than did the modelled torque, and was followed by an overshoot of negative torque during the resting phase prior to the next contraction (Figure 8.1.1). Section 7.2.2 hypothesised that this rapid decline in measured torque was the result of active deceleration by the ergometer control system and/or elastic recoil within the drive belt. This behaviour could not be accounted for within the present model, even with the addition of inertial effects from non-isokinetic crank rotation.

Despite the lack of fit between measured and modelled results during the declining phase, the model predicted the peak angle of stimulation cessation to be within 4 deg of the measured angle for the quadriceps muscle (refer to the next paragraph for qualification of this statement). This lends support to the accuracy of the model during the declining phase, because the timing of this torque decline is critical for the prediction of stimulation timing. It appears likely that the rapid decline in measured torque and subsequent overshoot were manifestations of the ergometer applying force to the pedals, while the muscles generated forces similar to those predicted by the model (see Section 7.2.2).

Peak stimulation firing angles

Peak stimulation firing angles were estimated by applying curve fitting techniques to measurements of average power output resulting from different stimulation firing angles. The resulting peak firing angles, however, were calculated with a very high degree of uncertainty. A number of reasons were discussed in Chapter 7 for the lack of precision in determining peak stimulation angles. A major reason was the relatively low sensitivity of power output to changes in stimulation firing angles when near their peak. Indeed, Section 7.2.3 suggests that changing quadriceps stimulation onset angle by 35 deg away from the peak would reduce average power output by less than 6%.

Computer simulations always estimated peak stimulation firing angles to be within the range of values given by the measured peak angles and the uncertainty in identifying those angles. Given the preceding statements about the precision of measured angles, this was not considered a strong corroboration of the model's predictive ability. Rather, support for the model comes from its ability to predict the patterns of torque production already discussed. Section 8.2 demonstrates that the direction of crank torque production immediately after stimulation onset determines which firing angle results in peak power output. If the model can predict how the timing, direction and magnitude of the early torque production changes with different stimulation firing angles, then it should also be able to predict the firing angles that would maximise power output.

8.2 NMES timing to generate maximum power output under acute conditions

Overview

Muscles can only do positive work on the crank when they are shortening. This is self-evident without considering the role of joint torques applying an external force to the pedals through inter-segmental dynamics. Rather, it can be deduced by considering whether a muscle generates or absorbs mechanical energy. By definition, positive work is done only during concentric contractions, when the moment generated by a muscle about a joint acts in the

same direction as the angular velocity of the joint (ie, when the power generated is positive. Winter, 1990). A muscle can only perform positive work on the crank when it generates energy; that is, while contracting concentrically.

Once the range of crank angles through which a muscle shortens has been identified, some allowance must be made for the time taken to change force levels in response to stimulation onset or cessation. After stimulation commences, there is a delay before a muscle begins to develop force. Once the muscle begins to develop force, there is a further period while the force rises to maximum levels. During this force rise, stimulation timing becomes a compromise between turning stimulation on early enough so that maximum force is generated during the concentric phase, and late enough to minimise the amount of negative crank torque generated while the muscle force is rising during the eccentric phase. This compromise can be seen in Figure 8.2.1, illustrating an ideal situation where a muscle generates maximum force instantaneously at the time when the muscle begins to shorten (Time A). This is compared with a more realistic muscle that takes time to generate tension and stimulation must therefore commence earlier at Time B. The compromise position for the realistic muscle is reached when the negative area before concentric shortening balances the reduction in work done by the realistic torque during the concentric phase. Earlier stimulation onset would reduce the loss during concentric activity, at the cost of increased negative work done before muscle shortening. Later stimulation onset would reduce the negative work done, but would also reduce the amount of positive work done during the concentric phase. This point has been previously explained by van Soest and Casius (2001).

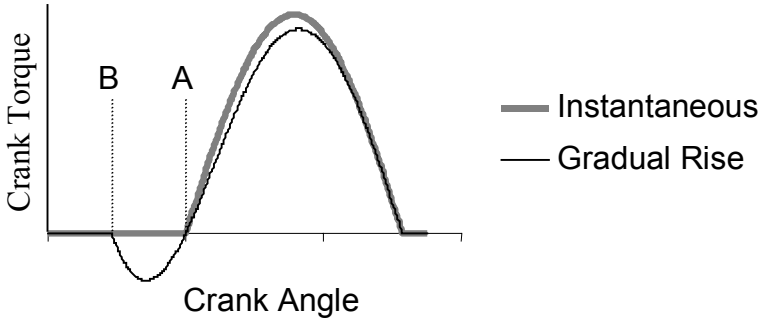

Figure 8.2.1 Idealised crank torque-angle curve (see text for details)

In summary, optimal stimulation timing requires knowledge of when the muscle shortens, and how long it takes to develop force after stimulation commences or ceases. The following paragraphs provide more specific details for each muscle group.

Quadriceps muscles

The quadriceps are comprised of four distinct muscles; three vastii muscles crossing only the knee joint, and rectus femoris that crosses both the hip and the knee. Because the vastii are single joint muscles, their direction of length change may be determined just from the action of the knee. Shortening of the vastii muscles occurs whenever the knee is extending. Rectus femoris is more complex because it crosses both the hip and knee joints, however the physiological cross sectional area of rectus femoris comprises only about 17% of the total quadriceps group (Section 2.4.5). Consequently, stimulation timing for the quadriceps group is dependent mostly on the actions of the vastii muscles, with little contribution from rectus femoris. Simulations suggest that stimulation of the quadriceps group as a whole begins to generate positive crank torque about 3 deg before the crank angle at which the vastii begin to shorten (Figure 8.2.2). This 3 deg advance is the result of rectus femoris beginning to shorten 27 deg earlier than the vastii. If only the vastii were contracted, then the instant they begin to shorten would coincide with the production of positive crank torque.

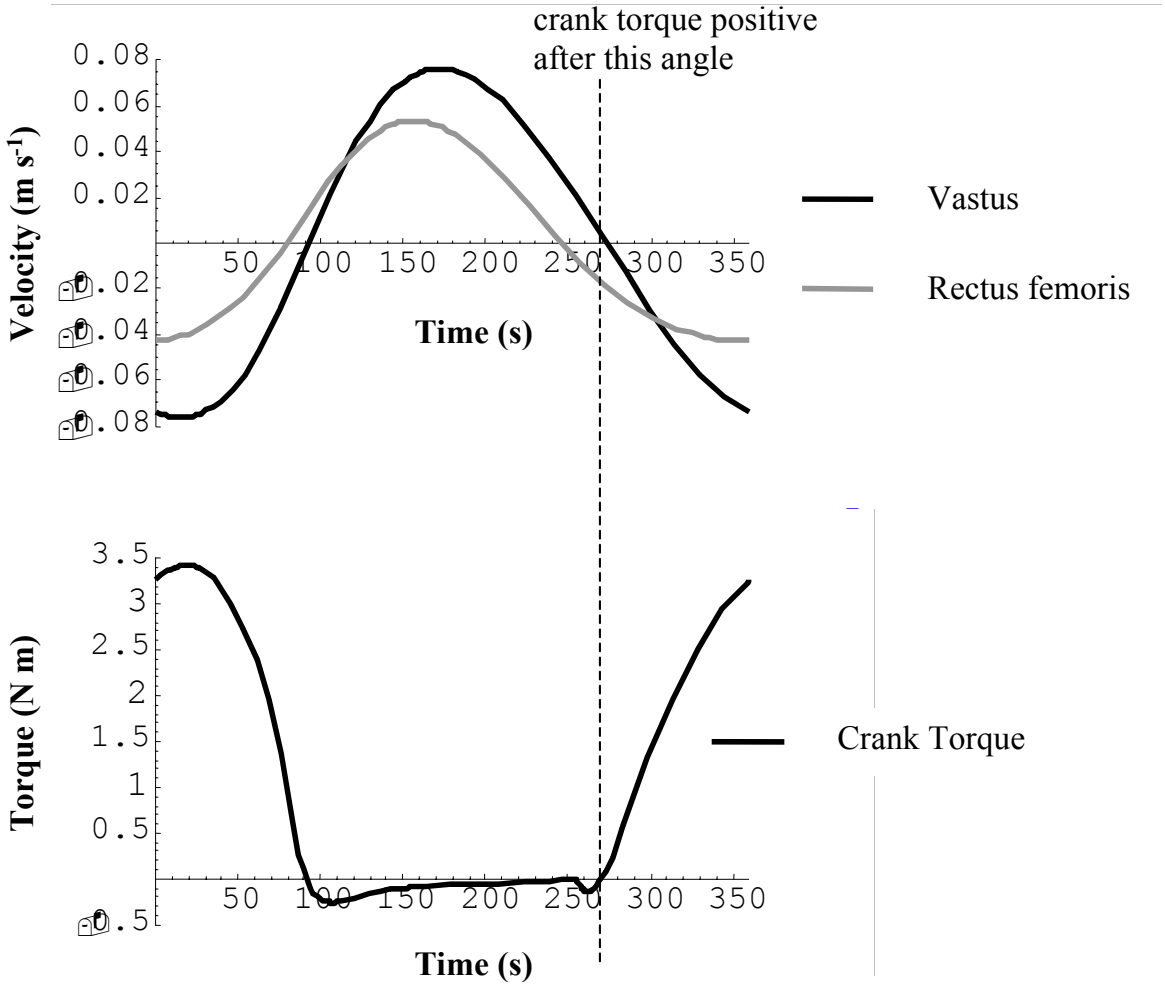

Figure 8.2.2 Simulated velocity of shortening and crank torque generated by the quadriceps muscles. Crank torque was simulated using the NMES firing angles of 235 and 52 deg that were calculated to generate maximum power output for a single exemplar subject.

Computer simulations determined that the stimulation onset angle resulting in maximum power applied to the crank was 235 deg. This was 35 deg before positive torque could be applied to the cranks by the quadriceps as a whole, and 38 deg before the vastii muscles commenced shortening. The pre-firing allows time for the muscles to generate tension before they are required to generate positive torque. At 50 rpm, 35 deg represents a delay of 117 ms; comprising 53 ms rise delay and a further 64 ms for muscle force to rise before the time positive crank torque can be applied by the muscle. This 53 ms delay time will be constant for all muscles within the present model because they were all modelled using the same delay constant.

There was very little difference in the timing of peak stimulation firing angles between individuals, with modelled peak onset and cessation angles within 3 deg for all subjects. Therefore, anthropometric variance between subjects did not produce the differences in timing patterns that were hypothesised in Section 1.1. Variations in leg lengths and proportionality caused differences in the range of knee angles through which each subject moved; however, the crank angles where knee extension commenced and ceased remained similar between subjects (Figure 7.5.2.2). Consequently, peak stimulation timing for the quadriceps was similar between subjects.

Gluteus maximus

Gluteus maximus is an extensor muscle that crosses only the hip joint. Therefore, all fibres of this muscle begin to shorten when the hip extends. The fibres of gluteus maximus are of different lengths with a range of moment arms and pennation angles (Friederich and Brand, 1990); however, all fibres must commence shortening at the same instant. The present model is limited in that it tries to represent the whole gluteus maximus with a single fibre. This limitation affects the model's ability to predict the amount of torque produced at different hip angles, but should have only limited effect on the timing of peak stimulation firing angles. Section 7.5 suggests that variables such as fibre length and pennation angle have a minor effect on peak stimulation angles, while moment arms have only a small effect on single joint muscles. The major limitation of the present model on the precise estimation of peak stimulation firing angles is estimation of tendon slack length. In order to provide some fit between in-vivo measurements and modelled torque-angle curves, the single fibre gluteus maximus model was given a tendon length of 0.05 m. It will be discussed below that longer tendon lengths require earlier stimulation firing in order to give time for the tendon to stretch. Tendon length was not found to greatly affect stimulation firing for the vastus muscle in Section 7.6, however slack length could not be changed by more than 10% without the single fibre model ceasing to work with the fibre producing zero force at either very long or short lengths. The anatomical structure of gluteus maximus may allow much larger ranges of tendon lengths with a distribution of fibres of greatly differing lengths, moment arms and tendon slack lengths

Simulations found the delay between peak gluteal stimulation onset and the generation of positive crank torque to be approximately 30 deg. Therefore, stimulation should commence at

a crank angle 30 deg before that at which hip extension commences. At 50 rpm, 30 deg represents a time of 100 ms, comprising of 53 ms rise delay and 47 ms force rise time.

Peak stimulation firing angles for gluteus maximus were constant between individuals, as they were for the quadriceps muscles. Again, each subject moved through different hip angles, however the crank angles producing maximum hip flexion and extension were relatively unchanged. Therefore, as for the quadriceps muscles, there appears to be no need to alter gluteal stimulation timing patterns between individual subjects.

Hamstrings

Being two joint muscles, the hamstrings begin to generate positive work not just when the hip or knee begin to extend, but when the whole muscle commences shortening. As discussed in Section 7.5.3, the timing of commencement of muscle shortening is dependent upon the angular velocities of the hip and knee and the relative moment arms of these joints. The findings reported within Sections 7.3 and 7.5.3 suggest that inter-individual differences in hip and/or knee moment arms produce different optimal timing sequences for individual subjects.

Simulations of hamstring function suggest that hamstring stimulation should commence approximately 40 deg in advance of the crank angle at which the hamstrings begin to shorten. This relative timing is consistent even for subjects having large differences in apparent hip-knee moment arm ratios, with consequent differences in the angles where hamstring shortening commences. At 50 rpm, the 40 deg advance firing represents 133 ms, comprising of 53 ms rise delay and a rise time of approximately 80 ms.

The present project has identified the largest range of crank angles over which muscle stimulation may be applied in order to maximise acute power output while cycling. For the quadriceps and gluteal muscles, this process required simply identifying the crank angles where the knee and hip began to extend and flex; then applying some timing advance to these identified crank angles. For the hamstring muscles, this process was not so simple because the muscles shorten at angles defined by the interaction between angular velocities of both the hip and knee, together with relative moment arms of the muscles across these joints. Further complications come from the finding that individual subjects may differ in their relative hip-knee moment arms, and consequently in the crank angles over which the hamstring muscles would shorten. This implies that, should a range of hamstring firing angles be specified over

approximately 180 deg as with the other muscles, there would be significant eccentric activity present in some subjects. Specifying specific hip-knee moment arm ratios for individual subjects would rectify this problem, however this limits the model's practical applications for novel subjects. In order to allow the model to predict useful stimulation firing patterns for all subjects it may be better to reduce the range of active angles to less than 180 deg.

Comparison of Timing between muscles

The preceding sections show that, once the crank angle where a muscle commences shortening has been identified, peak stimulation firing should commence a certain time in advance of that angle to allow time for the muscle to respond to the stimulation. Simulations with different crank angular velocities suggest that the *time* between stimulation onset and muscle shortening is consistent, regardless of crank velocity. Therefore, if cycling at half the crank velocity, the range of crank angles between stimulation onset and commencement of muscle shortening should also be halved.

Simulations also suggest that the peak stimulation timing differs between muscles, even though identical activation constants were used in the models for each muscle (Table 8.2.1). The models for each muscle group differed only in their optimum fibre length, tendon slack length and angle of pennation. Section 7.6 demonstrated that the models were not sensitive to pennation angle; hence, only fibre length and tendon slack length could explain the differences between the muscle models. A longer tendon length might require more time to extend the tendon at the commencement of each contraction before muscle force began to rise. The primary effect of fibre length would be that, since Hill's constant b is proportional to fibre length, a longer fibre would shorten more quickly; potentially allowing later stimulation firing.

Table 8.2.1 compares the fibre length and tendon slack length of each muscle model with the time duration between the peak onset of stimulation and commencement of muscle shortening. It appears that the amount of time duration may be related to tendon length more than fibre length, with a strong correlation existing between tendon slack length and stimulation timing for the three muscles examined ($R^2 = 0.95$). Fibre length, by contrast, does not change consistently with stimulation timing ($R^2 = 0.65$).

Table 8.2.1 Comparison of peak stimulation timing between muscles

	Hamstrings	Vastii	Gluteals
Stimulation firing time (ms)*	133	117	100
Tendon length (m)	0.385	0.156	0.05
Fibre length (m)	0.096	0.085	0.18

* Stimulation firing time represents the amount of time a muscle should be stimulated in advance of the time when that muscle begins to shorten.

8.3 Comparison of NMES firing angles from the present model with previously published values.

The present study used a novel ergometer (MOTOmed viva) with no previous research into suitable NMES firing angles. In order to compare the model's ability to predict timing patterns with prior research, the model was adjusted to mimic the seating position used for the ERGYS ergometer described in Section 1.1. Schutte (1992) has previously determined optimal NMES timing parameters for this ergometer using modelling methods similar to those of the present study. The anthropometric parameters of Schutte's model (leg length, seat position, etc) were used as inputs to the present model in order to compare predictions between models as well as to the firing angles used by the commercial ergometer.

Table 8.3.1 shows predictions by the present model using the MOTOmed ergometer for each muscle, averaged from all subjects in Chapter 7. These are compared to the present model matched to an ERGYS seating position using Schutte's (1992) anthropometric data, predictions made by Schutte's model and the firing angles used by the ERGYS ergometer. Predictions made by the present model for the quadriceps and hamstring muscles are similar

to those of Schutte, with the maximum difference being 15 deg for quadriceps onset angle. While it is difficult to quantify reasons for difference between models, it seems likely that these differences would result from a combination of tendon length, activation constants, moment arm and/or the ratio of rectus femoris to vastii muscle strength. Both models predicted firing angles that spanned those actually used by the ergometer.

Table 8.3.1 Comparison between NMES firing angles predicted by the current model and those published elsewhere.

	Current model (MOTOmed)	Current Model (ERGYS)	Schutte Model (ERGYS)	ERGYS angles
Quadriceps	236 - 53	252 - 68	237 - 73	308 - 23
Gluteus maximus	273 - 85	300 - 109	287 - 114	6 - 73
Hamstrings (standard model)	341 - 166	3 - 187	45 - 231	113 - 172
Hamstrings (knee moment arm reduced *)	293 - 122	322 - 155		
Hamstrings (knee moment arm increased #)	373 - 187	25 - 195		

Data represent NMES onset and cessation angles expressed with respect to TDC.

* Knee moment arm reduced by 40% to match the smallest moment arm fitted to an individual subject in Section 7.3.1.

\# Knee moment arm increased by 25% to match the largest moment arm fitted to an individual subject in Section 7.3.1.

Hamstring firing angles from Table 8.3.1 were more different between models. While both models again spanned those used by the ergometer, the model by Schutte (1992) predicted peak firing angles ranging more equally either side of those used by the ergometer. Modifying the present model by decreasing the hamstring moment arm about the knee shifted predicted peak firing angles towards those used by Schutte (1992). A reduction in hamstring moment arm about the knee from those initially modelled using data from Buford et al. (1997) was the most common result from the fitting procedure used in Section 7.3. This does not necessarily suggest that Buford et al. over estimated hamstring moment arms at the knee, simply that they were not in proportion to those measured at the hip by Visser et al. (1990). This may represent a result of using parameters derived from different studies, rather than from the measurement in any single study (see Section 6.1.7 for discussion).

The present model confirms earlier predictions by Schutte (1992) that NMES firing angles over approximately 180 deg would result in the greatest power output under acute conditions. The final section of this chapter will discuss how these predictions might differ when aiming to maximise power output over an extended period of cycling.

8.4 The ability of models to predict seat positions that maximise power output.

While the focus of this study has been on the development of stimulation patterns to control NMES cycling, musculoskeletal modelling has the potential enhance our understanding of other aspects of the activity. For example, Schutte et al. (1993) used modelling to identify seat positions that would minimise the muscle strength required to cycle at a given power output. Changing seat positions altered the range of joint angles through which individual subjects moved, with consequent changes in the torque and power generated by the muscles. To have confidence in predictions of this nature, a model must be capable of providing an accurate match to joint torque-angle curves throughout the full range of joint angles to be modelled.

There were a number of limitations identified within the present model that affected its ability to predict torque-angle curves for all muscles. Firstly, NMES cycling typically involves hip

and knee angles flexed beyond 90 deg. There is very limited data available for muscle moment arms as well as in-vivo measurements of joint torques beyond 90 deg of flexion, limiting the ability to make judgements about the model's ability through this range. Because moment arm estimations require extrapolation beyond the range of values measured experimentally, there is the potential for significant error within this range.

Secondly, relative hamstring moment arms at the hip and knee appear to vary between individuals. Figure 8.1.1 demonstrates that, even if the model produces accurate patterns of hip and knee torque in response to hamstring stimulation, the ratio of hip to knee moment arm magnitudes affects the shape of crank torque-angle curves. This would have consequences in the model's ability to predict factors like optimum seat position without individual adjustment of moment arms within the model.

Finally, isometric torque-angle curves for gluteus maximus were not well modelled by a single fibre, with consequent effects on the prediction of cycling torque curves (Sections 6.2.2 and 7.4.1). This would have particular limitations on the model's ability to predict such features as optimum seat position owing to a lack of confidence in the model's hip torque generated at different hip angles. It is not clear whether this limitation would also be extended to the model developed by Schutte (1992). Schutte's model matched in-vivo data much better than did the present model, however Section 6.2.2 suggests that the difference may be due to Schutte's model's parallel elastic element. It is difficult to compare the two models without knowing the relative contribution of active and passive elements to joint torques within Schutte's model. If, however, her model's hip extension torque at large angles of flexion was generated largely by passive elements, this would not necessarily give more accurate predictions regarding the generation of active torque and power through muscle stimulation. To improve predictions for the gluteus maximus muscle, it is suggested that future modelling use a number of different fibres within the model; each fibre having different lengths and/or moment arms. More anatomical research is required before such a model can be developed in order to provide detail of the range of lengths and moment arm patterns present within the muscle.

8.5 NMES timing to generate maximum power output over extended periods

Results and discussion within this thesis have concentrated on the ability of the model to predict stimulation firing angles that maximise power as an acute response to stimulation changes. The ideas developed and tested have looked at the average power output produced during a 10 s period, with no consideration of how this power output would change over time. The decision to delimit measurements to an acute response was taken deliberately. The aim was to test the model's ability to predict muscle forces in response to stimulation, and then take these muscle forces through the segments to generate external forces on the pedal.

Fatigue will decrease the force generating capacity of the muscles. It was shown in Section 5.1 that, while the magnitude of isometric knee extension torques declined by more than 75% with fatigue, the patterns of torque production remained quite consistent. There was no change in rise delay, rise time or fall delay; however the time for torque to decline after stimulation cessation did increase with fatigue. When the effect of fatigue on patterns of crank torque production during cycling was examined during a bout of five minutes continuous cycling (Section 7.1, Figure 7.1.2.2), there was no change in the pattern of torque production with fatigue. Again, the magnitude of torques declined substantially with repeated muscle stimulation, however there were no measurable changes in the time for torque to rise or fall in response to stimulation onset and cessation. It appears that any changes in knee extensor torque fall time, apparent during isometric knee extension contractions, were too small to significantly affect measured crank torque patterns.

Because the pattern of crank torque development remained constant, even after fatigue had caused a 50% decline in power output, the same stimulation firing angles that maximised power output of fresh muscles would also be expected to maximise power output of fatigued muscles[1]. This argument is based on power output measured over an acute period in the fresh state, compared to another acute period in the fatigued state, but cannot be extended to include the average power over an extended period of time lasting from one state to the other (eg for

an entire 45 min training session). It is likely that the stimulation firing angles that maximise power output during acute periods would result in a different rate of muscle fatigue over the session duration. This is firstly because a greater power output would require greater energy utilisation by the muscles, which would accelerate fatigue. A second effect comes from the finding that power output is maximised by using a wide range of NMES firing angles, with approximately 180 deg between stimulation onset and cessation. Narrowing this range of stimulation angles would allow a greater period of rest for the muscles between contractions, potentially reducing the rate of fatigue. This second explanation cannot be accepted without further analysis. Narrowing the range of stimulation angles would certainly provide a longer rest period between contractions, however this would also require a greater amplitude of torque production to achieve the same power output. It is not clear whether the longer rest period would provide a greater buffer against fatigue than the lesser peak torque required by the widest possible range of firing angles.

The present model can offer insights that help investigate this question. Simulations were performed for a single subject using contractions of just the quadriceps muscles at the optimum stimulation firing angles of 258 to 54 deg. The range of stimulation onset and cessation angles was then progressively narrowed at 10 deg increments, while the model's muscle strength was increased to maintain a constant power output for all simulations. Increasing the model's muscle strength would be equivalent to increasing stimulation current in an individual, although the relationship would not necessarily be linear. Figure 8.5.1 illustrates the results of these simulations. The increase in contraction force necessary to maintain constant power output with decreased range of stimulation firing angles is not linear, with initial narrowing of the firing angles from peak values requiring only small changes in muscle force to maintain constant power output. This is because, near the identified peak stimulation firing angles, the muscles are relatively ineffective at applying torque to the cranks (see Figures 7.2.3.3 and 7.2.4.1). Moving the stimulation firing angles away from the peak values therefore does not greatly reduce overall power output, requiring only a small increase in muscle force to compensate. For those angles where the muscles are most effective at applying torque to the cranks, however, further narrowing of the firing angles produces a

[1] The effect of fatigue during both the isometric and cycling experiments was only assessed over a duration of five minutes. While this period would be expected to exhibit the greatest decline in torque and power, it is possible that differing mechanisms of fatigue may change patterns of torque production and thus affect optimal firing angles over longer durations of cycling. Further research is required to confirm whether patterns of torque production continue to remain constant over longer durations of cycling.

relatively larger decrease in power output. This consequently requires larger muscle force changes to compensate.

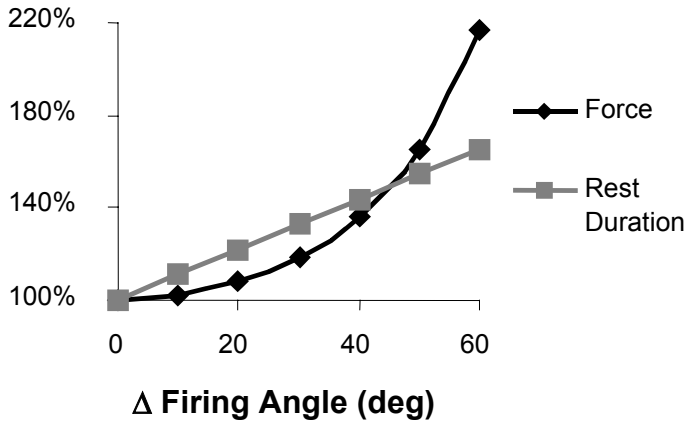

Figure 8.5.1 Effect of changing stimulation firing angles on the level of force required to maintain constant power output. Δ Firing Angle refers to a change in both stimulation onset and cessation angles from peak values. For example, data at 20 deg has a 40 deg narrower range of angles through which stimulation is active.

The effect of changing stimulation firing angles has been tested experimentally by Glaser et al. (1996). They modified the Ergys stimulation parameters by widening firing angles by 55 deg, increasing the maximum deliverable current from 140 to 300 mA, and adding stimulation of the tibialis anterior and triceps surae muscles. Cycling resistance was progressively increased by 1/16 kp increments at 2 min intervals until eight SCI subjects could no longer maintain a cycling cadence greater than 35 rpm. The maximum power output measured by Glaser et al. did not change, even with a substantial current increase. This suggests that any acute increases in power resulting from the widened firing angles may have been overshadowed by more rapid fatigue during the experiment. Acute responses were not reported by Glaser et al., only the maximum power output at the end of the step test.

The results of Glaser et al. (1996) could be interpreted as suggesting that the power output of SCI individuals' leg muscles may be limited by the physiological ability of the muscles to convert energy to external work, more than by the effectiveness of the stimulation protocol.

The present study demonstrates that power output during an acute phase may be increased by changes to the NMES firing pattern. Unless the rate of energy metabolism was similarly elevated, however, the muscles would not be able to sustain this increased work output throughout a training session.

Further analysis of the effects of widened stimulation angles throughout an entire training session cannot proceed without the inclusion of energy supply and demand within the muscle model. Models have been developed that predict energy utilisation under varying conditions of muscle force, length and velocity (eg Ma and Zahalak, 1991; Schutte, 1992). These models do not, however, consider the physiological processes required to release this energy. Therefore, they cannot predict the likelihood of a muscle being able to generate a particular energy consumption or how this consumption might change with fatigue.

While work is proceeding to generate models predicting fatigue rates for NMES contractions (eg Mizrahi, 1997), this process is not yet advanced enough to be useful for the current discussion. The current model only allows investigation of the acute force profiles that would be generated with changes in stimulation timing. While this does provide insights regarding the load induced by specific stimulation timing, further modelling is needed to predict responses to NMES over time. A complete model of the response to stimulation would have to include the effects of stimulation on electrolytic balances within the fibres, metabolic processes required to convert energy stores to external work and the ability of the blood supply to supply metabolites and remove waste products from the muscles. This would enable predictions to be made regarding optimum stimulation patterns for maximising power output over a full training session. This process could be extended even further to include, not only stimulation patterns that maximised power output throughout a training session, but also patterns that maximised muscle adaptations in response to training.